

Investigation of Double Slope Solar Distillation Efficiency using Heat Absorber Made from Zinc

Nattadon Pannucharoenwong^{1,*}, Phadungsak Rattanadecho¹,
Victoria Timchenko², Snunkhaem Echaroj¹
and Kriengkrai Nabudda³

¹ *Department of Mechanical Engineering, Thammasat University,
Pathum Thani 12120, Thailand.*

² *School of Mechanical and Manufacturing Engineering, The University of New South Wales,
Sydney 2052, Australia.*

³ *Department of Mechanical Engineering, Khon Kaen University,
Khon Kaen 40000, Thailand.*

Received 22 March 2019; Received in revised form 18 April 2019

Accepted 20 June 2019; Available online 31 October 2019

ABSTRACT

The productivity of water treatment through distillation method was studied by varying the size of the zinc heat absorber in a solar-based distillation unit. An additional zinc heat absorber was proposed to improve the efficiency of the distillation unit. This research investigates the usage of zinc heat absorber with size 10 to 90% of water surface area. The temperature at various locations inside the distillation unit was monitored throughout the operation in order to obtain data necessary for the equation engineering solver method, which was conducted to calculate the efficiency of the distillation system. It was found that the zinc heat absorber that is 10% of the water area produced 1.43 liters of condensed product per day providing efficiency of 25.99%. The efficiency reduced significantly to 15.02% when the size of the heat absorber was increased to 90%.

Keywords: Condensation unit; Heat absorber; Heat transfer solar energy.

1. Introduction

Pure distilled water has been used for many applications from laboratory to industry. However, water distillation is an energy intensive process which requires electricity and effective heat transfer. Application of solar radiation is a promising process for sustainable distillation of water without negative impact on the environment and residences in the area of the site. It is also economical and does not require advance manufacturing facilities. This research aims to develop an efficient water distillation unit to provide inexpensive distilled water using solar radiation to make local water refinery economically feasible. Solar radiation is an alternative energy process that is suitable for Thailand's concentrated high solar density capacity. Thermal heat from solar radiation can be used to boil water in a designed prototype distillation unit and condensed to be collected as distilled water. However, solar radiation efficiency in some areas is insufficient and requires a more effective distillation unit. Many different types of distillation units have been designed over the years including basin type solar stills, tilted tray design and vertical wick [1–3].

Over the years, many different designs have been proposed both as real models and in CFD simulations [4]. One of the most effective methods is to optimize heat output per unit area of the refiner [5]. A multi-level double-basin type still has been acknowledged among the high output per area distillation unit [6,7]. The major advantage of the multi-level type method is that latent heat contained in the vapor from the bottom layer is transferred to the water body of the upper layer [8,9]. Double-slope basin type stills have been employed as water distillation units in many cases. Kiwan et al. reported a reduction in system efficiency due to an increase in water's surface area inside the distillation still. An optimized height of the water pool area was also determined to optimize system

efficiency [10,11]. Maximum water production can be achieved at higher distillation temperature [12,13]. Phase change materials, such as paraffin wax and sodium sulphate, have been employed to enhance the effectiveness of the distillation unit [14,15]. Ionic liquids have also been employed to separate isopropanol from water which is a difficult procedure due to the very close boiling point of both substances [16,17]. Additionally, aluminum oxide nanofluid was also shown to significantly improve thermal efficiency [18,19]. Many other researches combined membrane technology with the distillation unit to obtain a superior separation mechanism but at a significantly higher cost [20,21]. Modi et al. reported a 18% increase in distillation efficiency when black cotton was used as a pile of wick and the water height was 0.01m [20]. Reddy et al. documented an increase in distillation efficient from 12.60 kg/d to 48.80 kg/d. When the process was conducted under a low-pressure and evaporative cooling condenser environment [18]. Singh et al. developed an improved photovoltaic thermal compound parabolic concentrator collector (PVT-CPC) [19]. Installation of a circular fin on the solar still was found to increase distillation productivity to 1.4917 kg/m²-day when the water depth is 0.01m. Another successful installation of a finned model was developed using black steel mesh fibers [21]. Financial analysis of general basin-type water distillation units was estimated in the range of from 0.035 to 0.074\$ per liter of distilled water [22]. Kalita et al. reported a maximum water yield of 3.94 liter per absorber area m² per day under solar radiation of 130 to 859 W/m² [23].

Solar radiation is a sustainable alternative source of energy that can provide reliable energy for a water distillation unit. The designed double-slope basin type distillation unit has a length of 1.5 m, width of 1 m and the water layer in each level was

20 cm, with one of the slope 14° . The upper layer of the distillation unit had increased surface. This research aims to investigate the effect of using zinc as the heat absorber. The area of the zinc heat absorber was varied from 10% to 90% of the basin.

2. Experimental Setup

2.1 Distillation unit design

A double-slope basin type distillation unit was designed for water distillation. As shown in Figure 1, the dimensions of the distillation under were generally 150 x 100 cm. and the water level was 20 cm. A water channel was installed in each level of the unit. Each section of the upper stage contained a varied surface area zinc heat absorber. The bottom stage of unit contained a panel of insulators and the glass slope made a 14° slope with the base of the unit.

2.2 Distillation operation

Data were collected during the 24 hours of operation. Solar intensity per hour, cumulative distilled water from each layer per day, and temperature variation inside the distillation unit were monitored. The surface area of the zinc heat absorber was varied from 10% to 90%. Temperature was monitored at different positions inside the distillation unit using a J-type thermocouple including ($T_{\text{atmosphere}}$, $T_{\text{insulator}}$, T_{glass2} , $T_{\text{water surface2}}$, T_{glass1} and $T_{\text{water surface1}}$) as shown in Figure 1. Approximately 75 liters of water was added to the bottom stage and 24 liters was added to the upper stage. The material used to make the heat absorber is zinc which is divided into different sized areas from 10% to 90% of the water surface area. The amount of distilled water was measured by using a volumetric flask, wind speed was monitored by using a flow meter, and wet/dry thermometers were used to measure temperature and relative humidity.

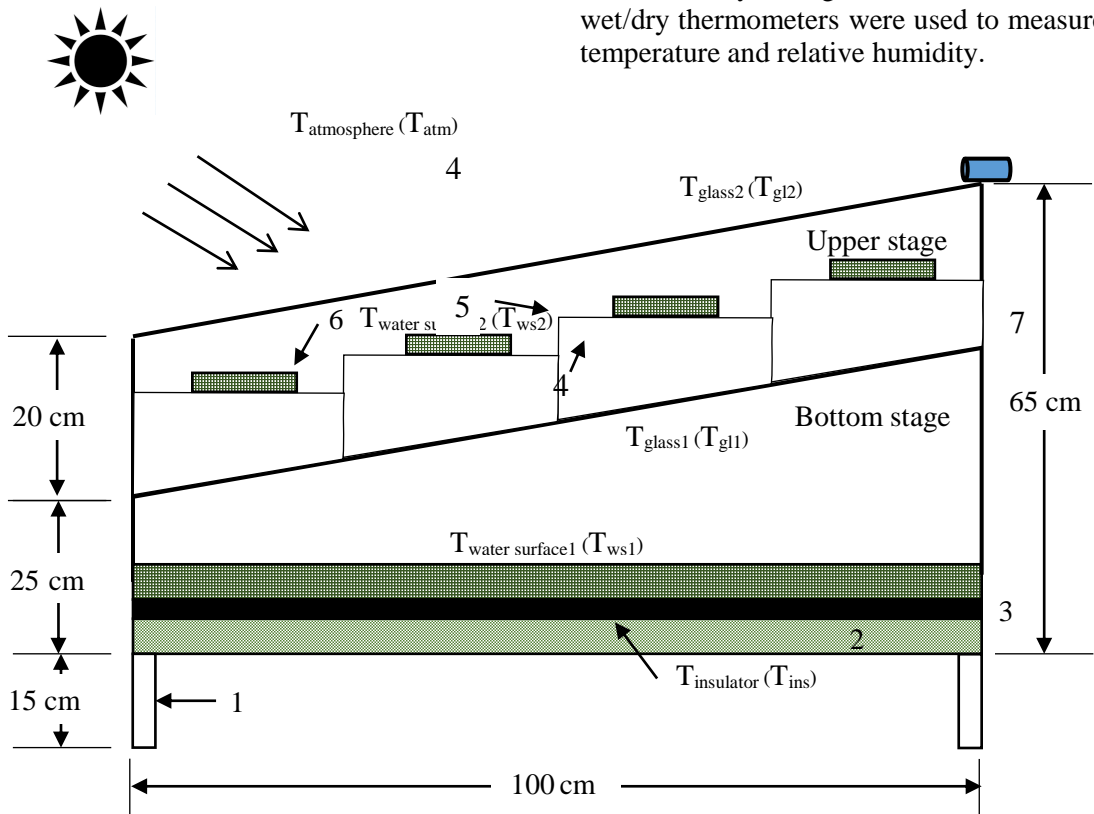


Fig. 1. Model of solar still water distillation. 1. Distillation leg stand, 2. Bottom wall, 3. Insulator, 4. Glass cover, 5. Upper gutter, 6. Heat absorber and 7. Inlet water.

2.3 Mechanism of water-base solar energy distillation

Heat is transferred from solar radiation through the glass layer that covers the upper stage of the distillation unit. The untreated body of water will also absorb the sun radiation, promoting evaporation. It is very important for the glass screen to be sloped in order to allow distilled or condensed water to be collected and flow down through the water gutter. Additionally, the length of the gutter needs to correspond to the dimension of the distillatory.

2.4 The Calculation of Solar Radiation

In order to calculate the solar radiation per hour (I_h), it is important to find the accumulated solar radiation per day (I_d)

and multiply it with total accumulated radiation in a day (r_{total}).

$$I_h = I_d \times r_{total} \tag{1}$$

$$r_{total} = \frac{\pi}{24} (a + b \cos \omega) \left[\frac{\cos \omega - \cos \omega_s}{\sin \omega_s - \left(\frac{2\pi \omega_s}{360}\right) \cos \omega_s} \right] \tag{2}$$

where $a = a_1 + a_2 \sin(\omega_s - 60)$ and $b = b_1 + b_2 \sin(\omega_s - 60)$, ω_s is the incidence angle between radiation ray and the area of strike level and values of a_1 , a_2 , b_1 , and b_2 , which depend on the location in Thailand. Since the experiment was conducted at Ubonratchathai station, the coefficient included $a_1 = 0.76$, $a_2 = -0.031$, $b_1 = 0.207$ and $b_2 = 0.238$.

Table 1. Energy balance equation at different locations inside the distillation unit.

| | |
|---------------------------------------|---|
| 1. Energy balance along the insulator | $m_{ins} C_{p,ins} \frac{dT_{ins.}}{dt} = I(t) A_{ins} - q_{ins} - q_{loss} \tag{3}$ <p>Where m_{ins} (10 kg) is the mass of insulator, $C_{p,ins}$ is heat capacity of insulator, T_{ins} is temperature of the insulator, A_{ins} is area of the insulator and q_{ins} is heat transfer from the insulator to the heat absorber.</p> |
|---------------------------------------|---|

| | |
|---|--|
| 2. Energy balance of water body at the bottom stage | $m_{ws1} C_{p,ws1} \frac{dT_{ws1}}{dt} = I(t) A_{ws1} + q_{ins} - q_{r,ws1} - q_{c,ws1} - q_{ev,ws1} \tag{4}$ <p>Where m_{ws1} is the mass of water in the bottom distillation still, $C_{p,ws1}$ (4,178 J/(kg°C)) is heat capacity of water in the bottom stage, A_{ws1} is equal to the water surface's area in the bottom stage, $q_{r,ws1}$ is heat transfer in radiation mode between water body and the cover of the bottom stage, $q_{c,ws1}$ is convective heat transfer and $q_{ev,ws1}$ is evaporation heat.</p> |
|---|--|

3. Energy balance of the glass surface in the bottom stage (5)

$$m_{gl1} C_{p,gl1} \frac{dT_{gl1}}{dt} = I(t) A_{gl1} + q_{r,gl1} + q_{c,gl1} + q_{ev,gl1} - q_{c,gl1ws2}$$

Where m_{gl1} (6 kg) is the mass of glass screen in the bottom stage, $C_{p,gl1}$ (800 J/(kg°C)) is heat capacity of glass screen in the bottom stage, T_{ws1} is temperature measured along the glass screen in the bottom stage, A_{gl1} represents glass screen's area in the bottom stage and $q_{c,gl1ws2}$ is the heat transfer from glass screen in the bottom stage to the water surface in the upper stage.

4. Energy balance of the water surface in the upper stage (6)

$$m_{ws2} C_{p,ws2} \frac{dT_{ws2}}{dt} = I(t) A_{ws2} + q_{c,gl1ws2} - q_{c,ws2gl2} - q_{r,ws2gl2} - q_{r,ws2gl2} + q_{HA}$$

Where m_{ws2} is the mass of water surface in the upper stage, $C_{p,ws2}$ is heat capacity of water surface in the upper stage, T_{ws2} is temperature of the water surface in the bottom stage, A_{ws2} represents the water surface's area in the bottom stage, $q_{c,gl1ws2}$ is the heat transfer from glass screen in the bottom stage to the water surface in the upper stage, $q_{c,ws2gl2}/q_{r,ws2gl2}/q_{r,ws2gl2}$ is heat transfer between water and glass screen in the upper stage of the distillation unit, and q_{HA} is heat transfer of the heat absorber.

5. Energy balance of glass screen in the upper stage (7)

$$m_{gl2} C_{p,gl2} \frac{dT_{gl2}}{dt} = I(t) A_{gl2} + q_{c,ws2gl2} + q_{r,ws2gl2} + q_{ev,ws2gl2} - q_{r,gl2atm} - q_{c,gl2atm}$$

Where m_{gl2} is the mass of glass screen in the upper stage, $C_{p,gl2}$ is heat capacity of glass screen in the upper stage, T_{gl2} is glass screen temperature in the bottom stage, A_{gl2} represents glass screen's area located in the bottom stage, $q_{c,ws2gl2}/q_{r,ws2gl2}/q_{ev,ws2gl2}$ is the heat transfer between water located in the upper stage to glass screen in the upper stage, $q_{r,gl2atm}$ is the heat transfer in radiation mode from glass screen in the upper stage to the atmosphere, and heat transfer in convective mode from glass screen in the upper stage to the atmosphere.

6. Accumulative distillation rate from both stages inside the unit (8)

$$\frac{dm_d}{dt} = h_{e,ws1gl1} \left[\frac{T_{ws1} - T_{gl1}}{h_{fg@T_{ws1}}} \right] + h_{e,ws2gl2} \left[\frac{T_{ws2} - T_{gl2}}{h_{fg@T_{ws2}}} \right]$$

Where m_d is the amount of accumulated distilled water produced over time, and $h_{e,ws1gl1}/h_{fg@T_{ws1}}/h_{fg@T_{ws2}}$ are heat transfer coefficients.

2.5 Transfer of heat inside the distillation unit

Energy loss during the heat transfer process usually represents an increase in cost and a decrease in the production of distilled water production rate. In addition to conduction and convection heat transfer, radiation also plays a significant role in the distillation process. Radiation can penetrate the glass screen of the distillation unit and can also be reflected from the glass screen into the water body. Radiation can also accumulate inside the system in the form of heat and be absorbed by the body of untreated water in the unit. Accumulated heat loss from the distillation unit included the following actions: Glass screen absorbed radiation, penetration of radiation through the glass screen, adsorption of radiation by untreated water, heat transfer in radiation mode from glass screen to the atmosphere, heat transfer in convection mode from glass screen to the atmosphere, heat transfer in radiation mode from untreated water to glass screen, heat transfer in convection mode from untreated water to glass screen, heat loss through the bottom/ sides of the distillation unit, heat loss during ventilation of the evaporative vapor steam and heat loss along the distilled water outlet.

Heat transfer and the amount of energy throughout the distillation unit can be calculated by energy balance in the distillation container as shown in Table 1.

2.6 Calculate heat transfer of the heat absorber object

The equation for finding the energy absorbed by the heat absorber is shown in equation 9.

$$q_{HA} = \alpha(I_a \tau_{sa} + I_s \tau_{ss}) \quad (9)$$

Where α represents the absorption in radiation mode by the material, I_a represents the hourly solar radiation impact on plane level, I_s represents the hourly distribution of

solar radiation on the plane level, τ_{sa} represents the transfer of solar radiation via steam absorption, τ_{ss} represents the transfer of solar radiation via steam scattering.

2.7 Calculating the efficiency of solar distillation unit

The equation for calculating the efficiency (η) of the distillation unit is shown in equation 10.

$$\eta = \frac{\sum \dot{m}_d h_{fg}}{\sum I} \quad (10)$$

Where \dot{m}_d is distillation rate, h_{fg} is latent heat and I is solar radiation condensation.

2.8 Calculation system

An EES computer based program is employed to find the efficiency of the distillation unit as shown in Figure 2. Some input parameters must be given in order to calculate the solar radiation equations (from equation 3 to equation 8) to obtain temperature values at each location inside the distillation unit ($T_{atmosphere}$, $T_{insulator}$, T_{glass2} , $T_{water\ surface2}$, T_{glass1} and $T_{water\ surface1}$). Variables demonstrated in the logical path for EES are required in order to calculate efficiency of the solar-base distillation and the temperature function to get the temperature values ($T_{atmosphere}$, $T_{insulator}$, T_{glass2} , $T_{water\ surface2}$, T_{glass1} and $T_{water\ surface1}$) as shown in equation 3-8.

Additionally, latent heat (h_{fg}) in the upper and bottom stage was employed to calculate for the distillation rate (productivity; m_d) and to figure out the the efficiency of the solar-based distillation system according to equation 10. Other input parameters are shown in the Table 2.

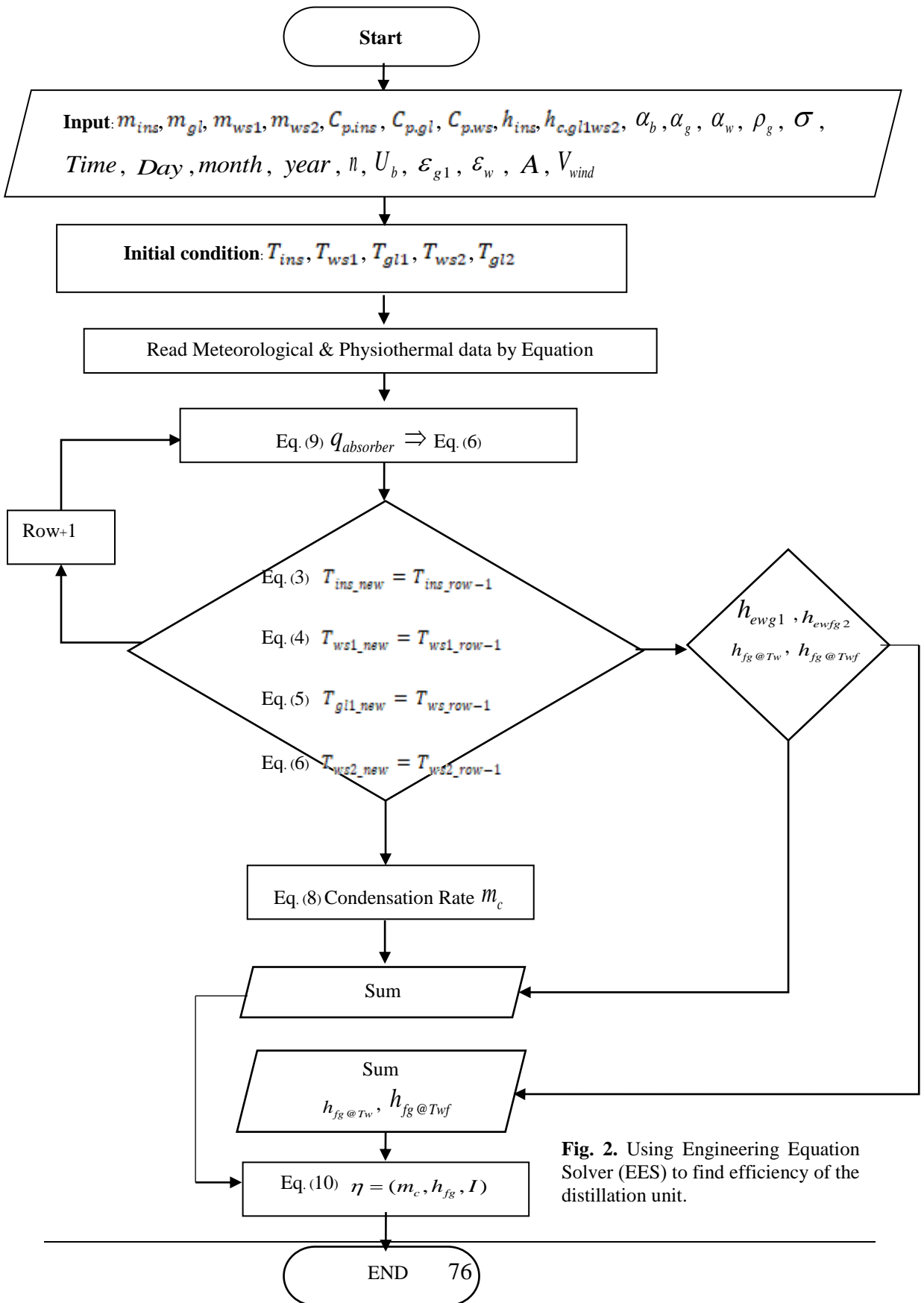


Table 2. Parameters for operating the double slanted-glass distillation unit [24].

| Operating conditions | Abrev. | Value | Unit |
|-----------------------------------|----------------|--------|-----------------------|
| Glass emissivity | ϵ_g | 0.88 | - |
| Water emissivity | ϵ_w | 0.96 | - |
| Radiation absorption of glass | α_g | 0.0475 | - |
| Radiation absorption of water | α_w | 0.05 | - |
| Reflectivity of glass | ρ_g | 0.0735 | kg/(cm ³) |
| Overall heat transfer coefficient | U_b | 14 | W/(m ² K) |
| Heat coefficient insulator | h_{ins} | 135 | W/(m ² K) |
| Convection coefficient | $h_{c.g11ws2}$ | 25 | W/(m ² K) |
| Wind velocity | V_{wind} | 3 | m/s |
| Thermal conductivity coefficient | k | 0.04 | W/(mK) |

3. Results and dicussion

3.1 Solar-based distillation unit

The aim of this experiment was to investigate the influences of zinc absorbers on heat transfer inside the distillation unit. The main parameter varied in this experiment was the size of the heat absorber, which was based on the area of the water surface from 10% of the area to 90% .Solar radiation was also monitored throughout the day from 8: 00 in the morning to 18:00 in the evening.

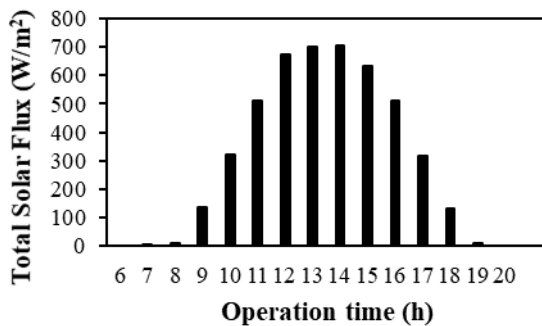


Fig. 3. Solar radiation condensation graphs.

3.2 Distribution of temperature inside the distillation unit

Temperature at different locations inside the distillation unit are shown in

Fig. 4. According to Fig. 4, it can be observed that temperature was maximized at 15:00 at all locations inside the distillation unit. The highest temperature measured was at the insulator which was installed at the bottom of the distillation unit. Temperature at the glass screen at the upper stage was the lowest compared with other locations inside the distillation unit. Water surfaces at the upper and bottom stage were slightly different. It was observed that the temperature difference between the glass screen of the bottom stage (T_{glass2}) and the water surface ($T_{water\ surface2}$) of the bottom stage was significantly higher than the temperature difference between the glass screen of the upper stage (T_{glass1}) and the water surface of the upper stage glass screen at the upper stage ($T_{water\ surface1}$). This was especially obvious after the operating hour passed 13:00. The temperature difference between the upper and bottom stage was the main driving force for the heat transfer process inside the distillation unit. The highest temperature difference between water surface and glass in the upper stage was approximately 7.10 °C, while the highest temperature difference for the bottom stage was 6.20 °C.

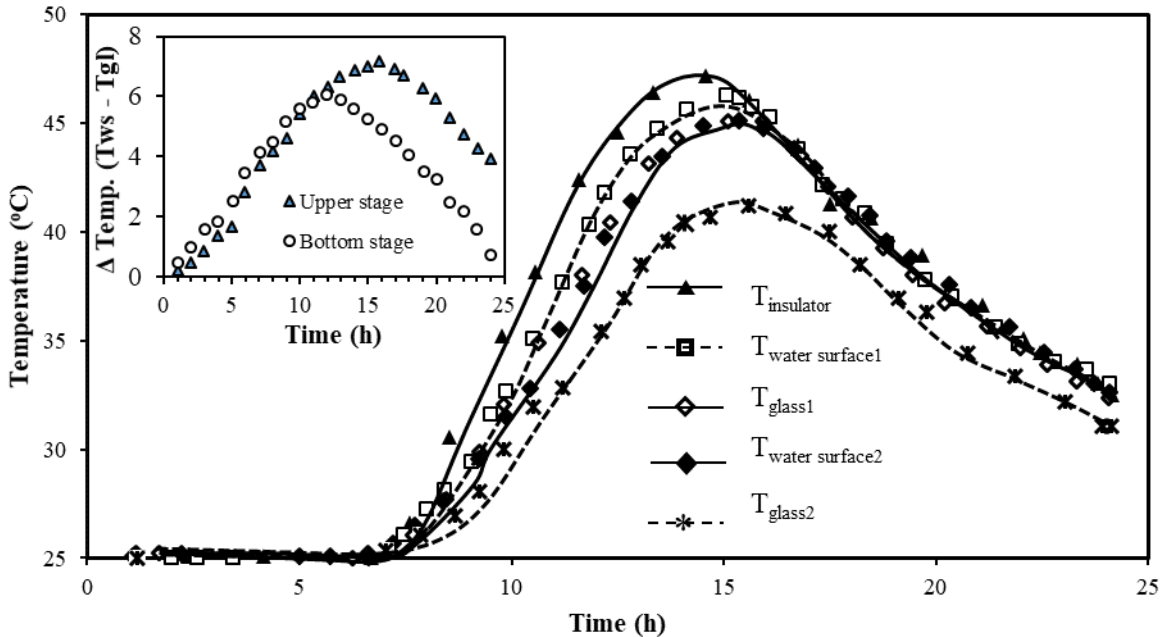


Fig. 4. Distribution of temperature at different location inside the distillation unit containing 10% zinc heat absorbers (inset: Temperature different between water surface and glass cover in each stage).

3.3 One day accumulation total productivity

Fig. 5 shows the accumulated amount of distilled water produced every hour from approximately 10:00. The total accumulated amount of distilled water was approximately 1.43 liters. The production rate of distilled water was highest from 10:00 to 16:00. The amount of distilled water collected from the upper stage continued to increase after 17:00, while the bottom stage stopped the production of distilled water after 17:00. The distillation rate as shown in the inset of Fig. 5 demonstrated the start of water distillation activity after 10:00 in the morning.

The upper stage was found to provide a higher distillation rate compared with the bottom stage due to the heat transfer gradient that resulted from the difference in glass screen and water surface temperature. The maximum distillation rate from the upper stage of the unit was approximately $0.26 \text{ g/s}\cdot\text{m}^2$, while the bottom stage had a distillation rate as low as $0.007 \text{ g/s}\cdot\text{m}^2$. Both stages provide the maximum distillation rate at 15:00. Water condensation did not take place before 09:00 due to insufficient energy for latent heat.

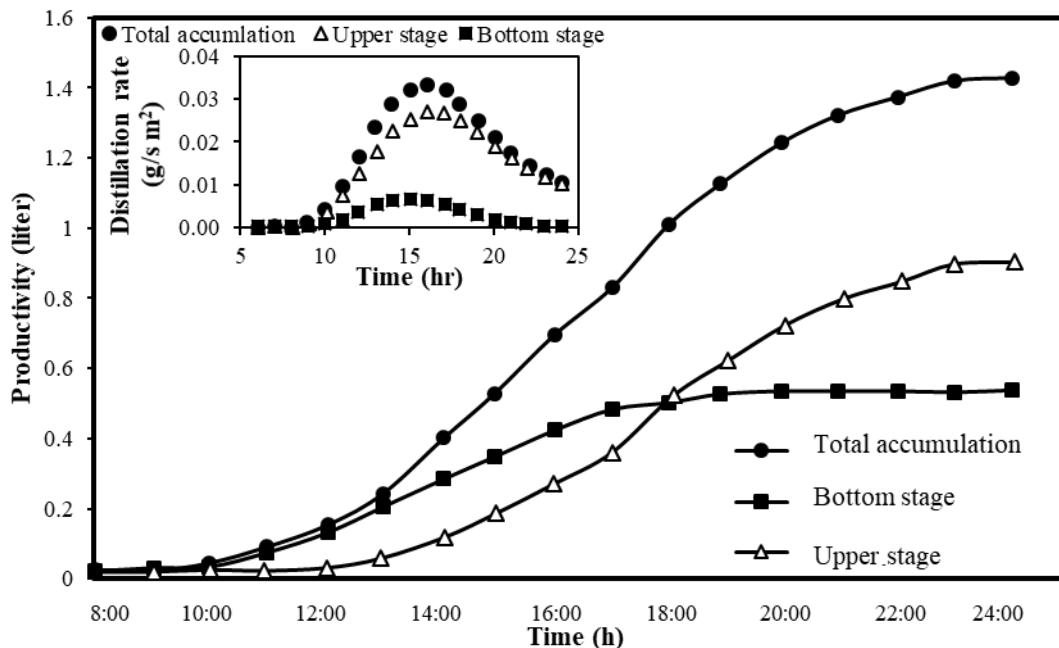


Fig. 5. Accumulation of distilled water produced within one operational day for distillation unit using 10% of zinc as heat absorber.

Production of treated water from the distillation unit was monitored in order to formulate the mathematical equation shown in equation 11. A polynomial of 6th order was proposed for this experiment. Prediction of the amount of distilled water generated was found to be very close to the data collected from the experiment as demonstrated by the R² value which is very close to 1 (0.997). This equation is capable of simulating the productivity by plugging in the operating time of the distillation set.

$$y = 4 \times 10^{-7}(P)^6 - 3 \times 10^{-5}(P)^5 + 0.0008(P)^4 - 0.0096(P)^3 + 0.0528(P)^2 - 0.1245(P) + 0.1111 \quad (11)$$

where P is the operating time of the distillation unit.

3.4 Influence of difference parameters on the distillation rate

Fig. 6 shows the effect of different parameters including wind speed, thermal conductivity of insulator, conductivity of heat absorber and water height on the distillation rate. It is observed that an increase in wind speed from 1 to 10 m/s corresponds with an increase in distillation rate. However, an increase in water height of the upper stage system was found to have an inverse effect on the distillation rate. This is because water can act as a barrier. Therefore an increase in the height of water may shield the solar heat transfer that could have been delivered to the heat absorber causing the distillation rate to diminish significantly from 8.2 liter/day to 4.6 liter/day. The thermal conductivity of the insulator also has the same relationship as the water height parameter. An increase in conductivity of the heat absorber seemed to have a slight positive effect on the distillation unit. The efficiency of the distillation unit is shown in Fig. 7. An increase in the size of the zinc heat absorber was found to decrease the efficiency of the distillation system.

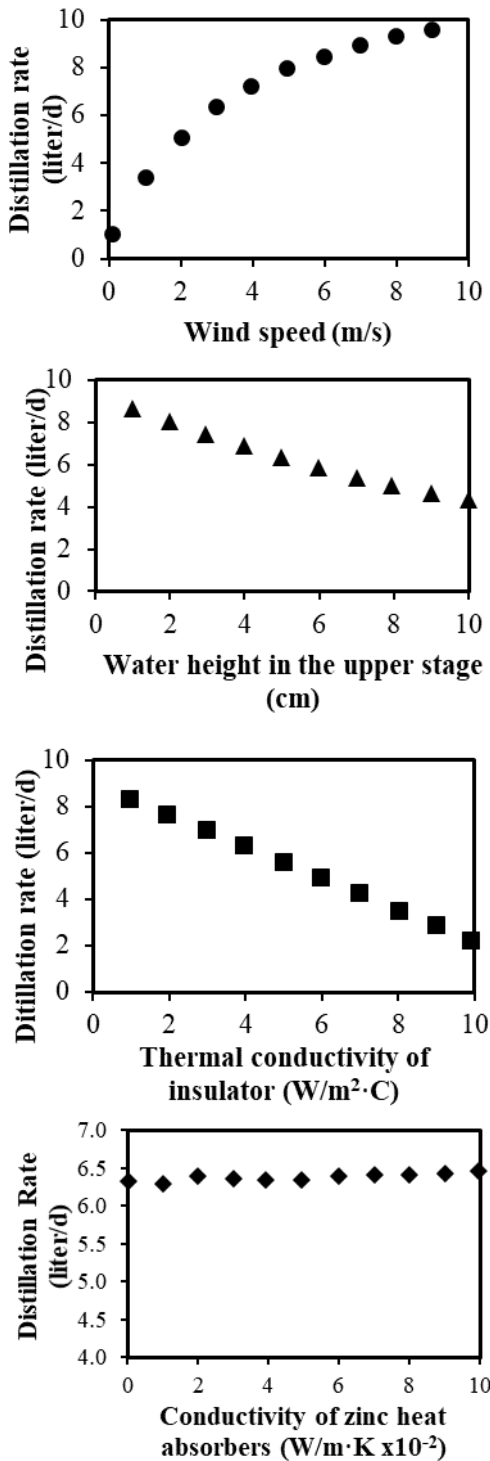


Fig. 6. Influence of different parameters (wind speed, water height, insulator thermal conductivity and heat absorber conductivity).

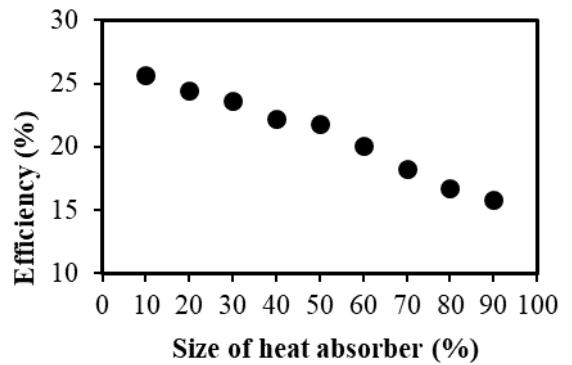


Fig. 7. Efficiency of the distillation unit calculated by using the EES procedure.

4. Conclusion

This experiment was conducted to investigate the effect of different parameters including wind speed, thermal conductivity of the insulator, heat absorber conductivity and weight height in the upper stage on the efficiency of the distillation unit. Collected data reveal a promising future for the distillation unit using zinc material as a heat absorber. An increase in area of the heat absorber was found to reduce the total productivity of the distillation unit from 1.43 liter per day to 0.92 liter per day. The highest efficiency achieved at heat absorber area of 10% was 25.99 %. Other parameters included wind speed, thermal conductivity of the insulator, and conductivity of the heat absorber. The productivity of distilled water was predicted through the 6th order polynomial equation with R^2 very close to 1.

Acknowledgements

The authors gratefully acknowledge the support of the department of Mechanical Engineering, the Faculty of Engineering, Khon Kaen University and Thammasat University who provided facilities in this study. The assistance and financial support from the Energy Management and Conservation Office (EMCO) are highly appreciated. The authors would also like to thank Kriengkrai Nabudda's research group for assisting with the experiment and data collection.

References

- [1] Kiwan S, Al-Nimr Md, Abdel Salam QI. Solar chimney power-water distillation plant (SCPWDP) . Desalination. 2018;445:105-14.
- [2] Al-Madhhachi H, Min G. Key factors affecting the water production in a thermoelectric distillation system. Energy Conversion and Management. 2018;165:459-64.
- [3] Gugulothu R, Somanchi NS, Devendar G, Deepika PKN. Solar Water Distillation Using Different Phase Change Materials. Materials Today: Proceedings. 2017;4(2, Part A):314-21.
- [4] Echaroj S, Pannucharoenwong N, Vengsungnle P, Wichangarm M. Effect of Geometric Design on Airflow Simulation Inside the Storage Room for Paddy. IOP Conference Series: Materials Science and Engineering. 2019;501:012040.
- [5] Vengsungnle P, Jongpluempiti J, Pannucharoenwong N, Echaroj S, Wichangarm M, Benjapiyaporn C, et al., editors. Evaluation of Mill Quality by Analysis of the Ventilation Behavior of Silo Blower. 2018 IEEE 5th International Conference on Engineering Technologies and Applied Sciences (ICETAS); 2018 22-23 Nov. 2018.
- [6] Ma S, Shang X, Zhu M, Li J, Sun L. Design, optimization and control of extractive distillation for the separation of isopropanol-water using ionic liquids. Separation and Purification Technology. 2019;209:833-50.
- [7] Elango T, Kannan A, Kalidasa Murugavel K. Performance study on single basin single slope solar still with different water nanofluids. Desalination. 2015;360:45-51.
- [8] Vengsungnle P, Jongpluempiti J, Pannucharoenwong N, Echaroj S, Wichangarm M, Benjapiyaporn C, et al., editors. Energy Saving from Heat Recovery in Paddy Drying Process. 2018 IEEE 5th International Conference on Engineering Technologies and Applied Sciences (ICETAS); 2018 22-23 Nov. 2018.
- [9] Pannucharoenwong N, Worasaen A, Benjapiyaporn C, Jongpluempiti J, Vengsungnle P. Comparison of Bio-Methane Gas Wobbe Index In Different Animal Manure Substrate. Energy Procedia. 2017;138:273-7.
- [10] Khatun; A, Rahman; MM, Alam S. Heat Transfer Characteristics of Nanofluid Due to a Permeable Rotating Disk with Slip Effect and Thermophoresis Science & Technology Asia. 2019;24:1-13.
- [11] Khan EU, Nordberg Å. Membrane distillation process for concentration of nutrients and water recovery from digestate reject water. Separation and Purification Technology. 2018;206:90-8.
- [12] Rahimpour MR, Kazerooni NM, Parhoudeh M. Chapter 8 - Water Treatment by Renewable Energy-Driven Membrane Distillation. In: Basile A, Cassano A, Figoli A, editors. Current Trends and Future Developments on (Bio-) Membranes: Elsevier; 2019. p. 179-211.
- [13] Echaroj S, Pannucharoenwong N, editors. Bioethanol production through enzymatic saccharification and fermentation of mechanically milled empty palm bunch. 2018 IEEE 5th International Conference on Engineering Technologies and Applied Sciences (ICETAS); 2018 22-23 Nov. 2018.
- [14] Khalifa AE, Alawad SM. Air gap and water gap multistage membrane distillation for water desalination. Desalination. 2018;437:175-83.
- [15] Jongpluempiti J, Vengsungnle P, Pannucharoenwong N. Investigation of parameters affecting cotton waste shredding for as straw mushroom substrates. Asia-Pacific Journal of Science and Technology. 2019;24,1-8.
- [16] Modi KV, Modi JG. Performance of single-slope double-basin solar stills with small pile of wick materials. Applied Thermal Engineering. 2019;149:723-30.
- [17] Jongpluempiti J, Pannucharoenwong N, Benjapiyaporn C, Vengsungnle P. Design and Construction of the Flat Plate Solar Air Heater For Spray Dryer. Energy Procedia. 2017;138:288-93.

- [18] Reddy KS, Sharon H. Energy-environment-economic investigations on evacuated active multiple stage series flow solar distillation unit for potable water production. *Energy Conversion and Management*. 2017;151:259-85.
- [19] Gupta VS, Singh DB, Mishra RK, Sharma SK, Tiwari GN. Development of characteristic equations for PVT-CPC active solar distillation system. *Desalination*. 2018;445:266-79.
- [20] Jani HK, Modi KV. Experimental performance evaluation of single basin dual slope solar still with circular and square cross-sectional hollow fins. *Solar Energy*. 2019;179:186-94.
- [21] Kalita P, Borah S, Das D. Design and performance evaluation of a novel solar distillation unit. *Desalination*. 2017;416:65-75.
- [22] Yousef MS, Hassan H. Energetic and exergetic performance assessment of the inclusion of phase change materials (PCM) in a solar distillation system. *Energy Conversion and Management*. 2019;179:349-61.
- [23] Muftah AF, Alghoul MA, Fudholi A, Abdul-Majeed MM, Sopian K. Factors affecting basin type solar still productivity: A detailed review. *Renewable and Sustainable Energy Reviews*. 2014;32:430-47.
- [24] Kalita P, Borah S, Das D. Design and performance evaluation of a novel solar distillation unit. *Desalination*. 2017;416:65-75.